

## Research Article

# Preparation of Hierarchical CaSO<sub>4</sub> Whisker and Its Reinforcing Effect on PVC Composites

Pengyang Ma,<sup>1</sup> Haoyuan Chen,<sup>1</sup> Qingjie Zhang,<sup>1</sup> Jing Wang<sup>1,2</sup> and Lan Xiang<sup>1</sup>

<sup>1</sup>Department of Chemical Engineering, Tsinghua University, Beijing 100084, China

<sup>2</sup>Key Laboratory of Synthetic and Biological Colloids, Ministry of Education, School of Chemical and Material Engineering, Jiangnan University, Wuxi 214122, China

Correspondence should be addressed to Jing Wang; wangjingflotu@gmail.com and Lan Xiang; xianglan@mail.tsinghua.edu.cn

Received 6 December 2017; Accepted 1 April 2018; Published 7 May 2018

Academic Editor: Stefano Bellucci

Copyright © 2018 Pengyang Ma et al. This is an open access article distributed under the Creative Commons Attribution License, which permits unrestricted use, distribution, and reproduction in any medium, provided the original work is properly cited.

CaSO<sub>4</sub> whiskers (CSW) can be used to reinforce PVC matrix to produce light and strong composites. However, the weak interfacial interaction between the smooth CSW and PVC matrix limited the fabrication of PVC composite with perfect mechanical properties. In this work, CaCO<sub>3</sub> nanoparticles were coated on CSW surface by wet modification of CSW in Na<sub>2</sub>CO<sub>3</sub> solution at 80°C, which increased the surface roughness of CSW from 56.8 nm to 115.6 nm. The use of the hierarchical CSW rather than the raw CSW in the fabrication of CSW/PVC composite led to the increase of the flexural strength from 86.3 MPa to 113.2 MPa and the impact strength from 56.7 kJ·m<sup>-2</sup> to 82.5 kJ·m<sup>-2</sup> owing to the enhanced mechanical interlocking between CSW and PVC matrix.

## 1. Introduction

Polyvinyl chloride (PVC) is one of the most commercially important polymers used extensively in various fields as pipes, doors, windows, floors, packaging, electric cables, and so on, owing to its high mechanical strength, high thermal stability and corrosion resistance, excellent electrical insulation, and relatively low cost [1–4]. The mechanical properties of PVC can be significantly improved by using appropriate inorganic fillers or reinforcing agents such as calcium carbonate, silica, carbon nanotube, and calcium sulfate whiskers (CSW) [5–7]. CSW are fiber-shaped single crystals with many desirable properties such as high aspect ratio, high strength and stiffness, nontoxicity, and low cost, making them the excellent fillers for polymers [8–12]. For example, it was reported that the frictional wear resistance of nitrile butadiene rubber (NBR-) modified phenol formaldehyde (PF) was improved by adding CSW and aramid fibers [9]; the presence of 15 wt% of CSW in the polycaprolactone composite led to the increase of 21% of flexural strength and 22% of the impact strength [10]; the tensile strength of polypropylene (PP) reached up to 37.6 MPa after filling 10 wt% of CSW [11]; the breaking strength, tensile modulus, and elongation of PVC composites

increased up to 53.5 MPa, 1772 MPa, and 225%, respectively, after filling 5 wt% of CSW [12].

The surface modification of CSW was usually adapted to improve the compatibility between CSW and the polymer matrix [13–16]. For example, the modification of CSW with sodium stearate led to the increase of the tensile strength of polypropylene (PP) composite containing 30 wt% of CSW from 19.2 MPa to 35.2 MPa [13]; the modification of CSW with glutaraldehyde crosslinked chitosan (GACS) led to the increase of the tensile strength and impact strength of the PVC composite containing 12 wt% of CSW by 17.5% and 40.4%, respectively [14].

Inorganic filler with high surface roughness (which can be achieved by many methods as plasma pretreatment, acidic or alkaline corrosion, surface modification, etc.) favored the interfacial interaction between the filler and matrix [17–20]. For example, it was reported that the coating of aramid fibers with multiwall carbon nanotubes led to the increase of the roughness of aramid fibers (AFs) from 3.2 nm to 21.3 nm and the increase of the interfacial shear strength of the AFs/polypropylene (PP) composite by 17% owing to the enhanced mechanical interlocking between the coated AFs and PP matrix [17]. Up to now little work was reported on

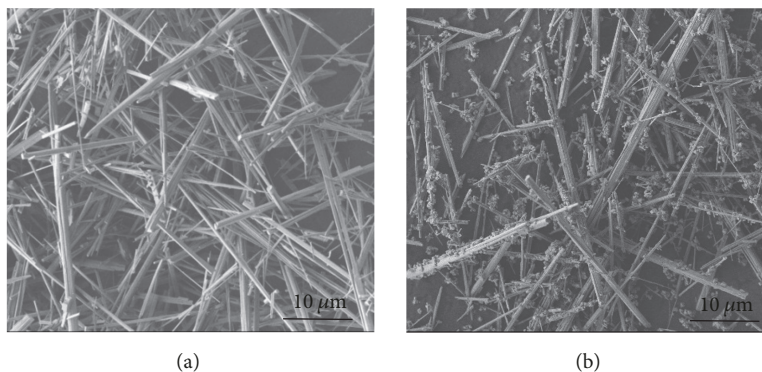


FIGURE 1: SEM images of CSW before (a) and after (b) modification.

the preparation of hierarchical CSW and their application in PVC composites was still unknown.

In this paper, hierarchical CSW, one-dimensional  $\text{CaSO}_4$  whiskers coated by zero-dimensional  $\text{CaCO}_3$  nanoparticles, were prepared via wet modification of CSW in  $\text{Na}_2\text{CO}_3$  solution. The influences of the hierarchical CSW on the interfacial and mechanical properties of the PVC composites were investigated.

## 2. Experimental

**2.1. Preparation of Hierarchical CSW.** Commercial chemicals with analytical grade were used in the experiments. 5.00 g of CSW with diameters of 2–4  $\mu\text{m}$  and lengths of 150–350  $\mu\text{m}$  was mixed with 500 ml of 0.03  $\text{mol}\cdot\text{L}^{-1}$   $\text{Na}_2\text{CO}_3$  solution at 80°C. After being stirred for 2.0 h, the slurry was filtrated, washed with deionized water, and dried in the furnace at 105°C for 12.0 h.

**2.2. Preparation of CSW/PVC Composites.** CSW/PVC composites were prepared by the compression molding method. 5.00 g of CSW or hierarchical CSW was mixed at 60°C with 50 ml of the solution containing 90 wt% alcohol and 1 wt% APS. After being stirred at 60°C for 4.0 h, the slurry was filtrated, washed with deionized water, and dried in the furnace at 105°C for 12.0 h. Then the modified CSW, PVC (with an average polymerization degree of 650–750), heat stabilizer, and stearic acid were mixed with a weight ratio of 30:70:4:1 in the high-speed mixer (FFJ-05, Chuangjia, China) at 5000  $\text{min}^{-1}$  for 5.0 min. The powders were then mixed at 175°C for 6.0 min in the torque rheometer (RM-200A, Harpo, China). After being broken in a vibratory crusher (FM-1, Yetuo, China), the particles were put into the vulcanizing equipment (ZG-50T, Zhenggong, China) and compression molded at 180°C and 20 MPa for 8.0 min to prepare the composite plate with a size of 200 × 150 × 10  $\text{mm}^3$ . Then the compression mold was cooled down to room temperature at 20.0 MPa.

**2.3. Characterization.** The morphology of the samples was examined with the field emission scanning electron microscope (FESEM, JSM 7401F, JEOL, Japan), the high resolution transmission electron microscopy (HRTEM, JEM-2010,

JEOL, Japan), and the atomic force microscopy (AFM, SPM-9600, SHIMADZU, Japan). The structures of the samples were characterized by the powder X-ray diffractometer (XRD, D8 advanced, Bruker, Germany) using  $\text{Cu K}\alpha$  radiation ( $\lambda = 1.54178 \text{ \AA}$ ) and the Fourier transform infrared spectroscope (FT-IR, Nicolet 670, Thermo Fisher, USA). The flexural and impact strengths of the composites were measured by the universal testing machine (ZWICKZ005, Jiuge, Shanghai). Ten specimens were tested for each data point, and then the average value was considered as the tested value.

## 3. Results and Discussion

**3.1. Morphology and Composition of Hierarchical CSW.** Figure 1 shows the SEM images of CSW before and after modification. Compared with the smooth surface of the CSW without modification (Figure 1(a)), hierarchical CSW coated with nanoparticles (with an average size of 50–100 nm) formed after modification of the CSW in 0.03  $\text{mol}\cdot\text{L}^{-1}$   $\text{Na}_2\text{CO}_3$  solution at 80°C for 2.0 h (Figure 1(b)). Figure 2 shows the HRTEM image of the hierarchical CSW. The nanoparticles were contacted closely with the CSW surface. Two kinds of interpenetrating lattices occurred at the interface of CSW and nanoparticles: the interplanar spacing of 0.174 nm which was corresponding to (040) plane of  $\text{CaSO}_4$  and the interplanar spacing of 0.302 nm which was corresponding to (104) plane of  $\text{CaCO}_3$ , indicating the formation of  $\text{CaCO}_3$  nanoparticles on CSW surface. Figure 3 shows the AFM 3D images of CSW before and after modification. The surface of the hierarchical CSW was much rougher than that of the raw CSW without modification, and the surface roughness values which were calculated from the topography images using AFM software increased from 56.8 nm for the raw CSW to 115.6 nm for the hierarchical CSW.

Figure 4 shows the XRD patterns and FT-IR spectra of the raw CSW and the hierarchical CSW, respectively. The data in Figure 4(a) showed that, compared with the raw CSW composed of sole  $\text{CaSO}_4$ ,  $\text{CaCO}_3$  phase occurred in the hierarchical CSW, which should be attributed to the coating of the  $\text{CaCO}_3$  nanoparticles on CSW surface. As shown in Figure 4(b), the FT-IR peak located at 2506  $\text{cm}^{-1}$  was attributed to the vibration of  $\text{C}=\text{O}$  in  $\text{CO}_3^{2-}$ , the peak at 1796  $\text{cm}^{-1}$  was assigned to the vibration of  $\text{C}-\text{Ca}$ , and the peak at 711  $\text{cm}^{-1}$

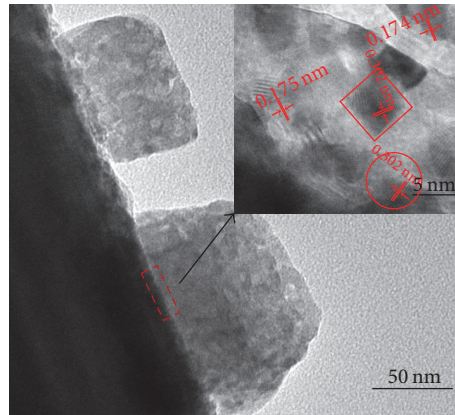


FIGURE 2: HRTEM of hierarchical CSW.

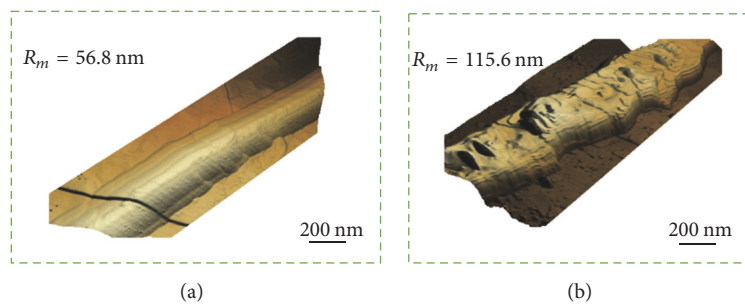


FIGURE 3: AFM 3D images of CSW before (a) and after (b) modification.

was connected with the deformation vibration of  $\text{CO}_3^{2-}$  [21]. The peaks at  $981\text{ cm}^{-1}$  and  $1022\text{ cm}^{-1}$  were connected with the symmetric stretchings of  $\text{SO}_4^{2-}$ . FT-IR analysis reconfirmed the coexistence of  $\text{CaCO}_3$  with CSW in hierarchical CSW.

Figure 5 shows the schematic drawing for the formation of hierarchical CSW in  $\text{Na}_2\text{CO}_3$  solution.  $\text{CaCO}_3$  nanoparticles may be coated on CSW surface via surface reaction or/and dissolution-deposition routes. That is to say,  $\text{CO}_3^{2-}$  in  $\text{Na}_2\text{CO}_3$  solution may react with  $\text{Ca}^{2+}$  on CSW surface, leading to the coating of  $\text{CaCO}_3$  nanoparticles on CSW surface:  $\text{CaSO}_4 + \text{Na}_2\text{CO}_3 = \text{CaCO}_3 + \text{Na}_2\text{SO}_4$ ;  $K_{298\text{K}} = 2.71 \times 10^3$ ; CSW may also dissolve partially in  $\text{Na}_2\text{CO}_3$  solution, and then  $\text{Ca}^{2+}$  and  $\text{CO}_3^{2-}$  in solution reacted and formed  $\text{CaCO}_3$  nanoparticles on CSW surface.

**3.2. Mechanical Properties of PVC Composites.** Figure 6 shows the effects of whisker content on the flexural strengths and impact strengths of the raw CSW/PVC composite and the hierarchical CSW/PVC composite. The reinforcing trend of raw CSW and hierarchical CSW in the composites' mechanical properties showed an inflection point at 30 wt% whisker content. In this case, the flexural strengths of raw CSW/PVC and hierarchical CSW/PVC composites were 86.3 MPa and 113.2 MPa, respectively, and the corresponding impact strengths were  $56.7\text{ kJ}\cdot\text{m}^{-2}$  and  $82.5\text{ kJ}\cdot\text{m}^{-2}$ , respectively. Compared with the raw CSW/PVC composite, the hierarchical CSW/PVC composite exhibited an increase of 31.2%

in the flexural strength and an increase of 45.5% in the impact strength, which should be attributed to enhanced interfacial interaction between the hierarchical CSW and PVC matrix. Significantly, in this present work, the optimal flexural strength and impact strength of hierarchical CSW reinforced PVC composites showed a remarkable value compared with that of the CSW modified by the glutaraldehyde crosslinked chitosan (77.5 MPa) [14] or the titanate coupling agent ( $15.9\text{ kJ}\cdot\text{m}^{-2}$ ) [15].

The morphology of the fracture surfaces of the raw CSW/PVC and the hierarchical CSW/PVC composites is shown in Figure 7. The cracks and the debonding whiskers occurred on the fracture surface of the raw CSW/PVC composite (Figure 8(a)) due to the poor interfacial adhesion between the smooth CSW and the PVC matrix, while CSW whiskers were connected closely with PVC matrix on the fracture surface of the hierarchical CSW/PVC composite (Figure 8(b)) owing to the enhanced interfacial adhesion between the hierarchical CSW and the PVC matrix.

**3.3. Interfacial Analysis of CSW/PVC and Hierarchical CSW/PVC Composites.** Figure 8 shows the micromechanical models for CSW/PVC and hierarchical CSW/PVC composites. The micromechanical model for CSW/PVC composite can be described as a single cylindrical whisker surrounded by PVC matrix (Figure 8(a)). The whisker would be pulled out of

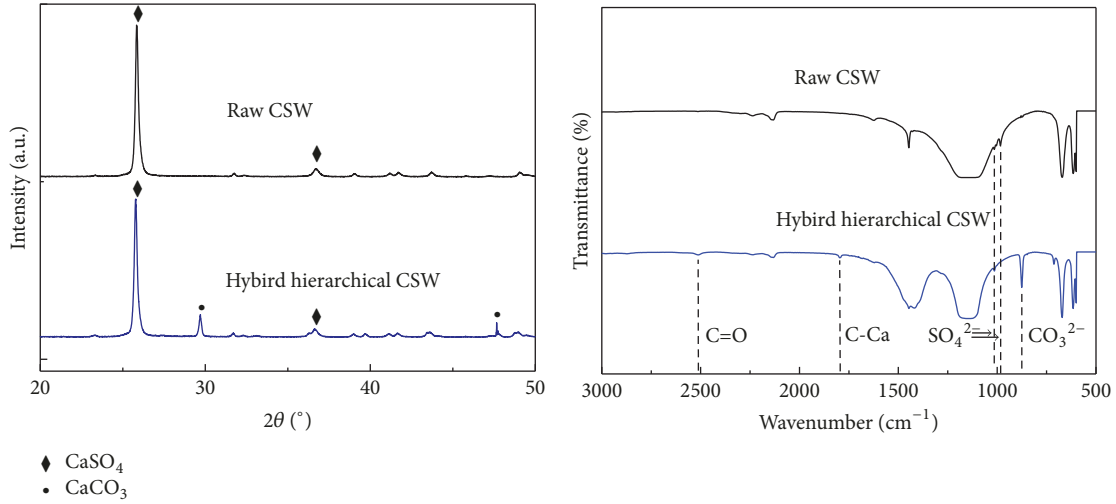


FIGURE 4: XRD (a) and FT-IR (b) of raw CSW and hierarchical CSW.

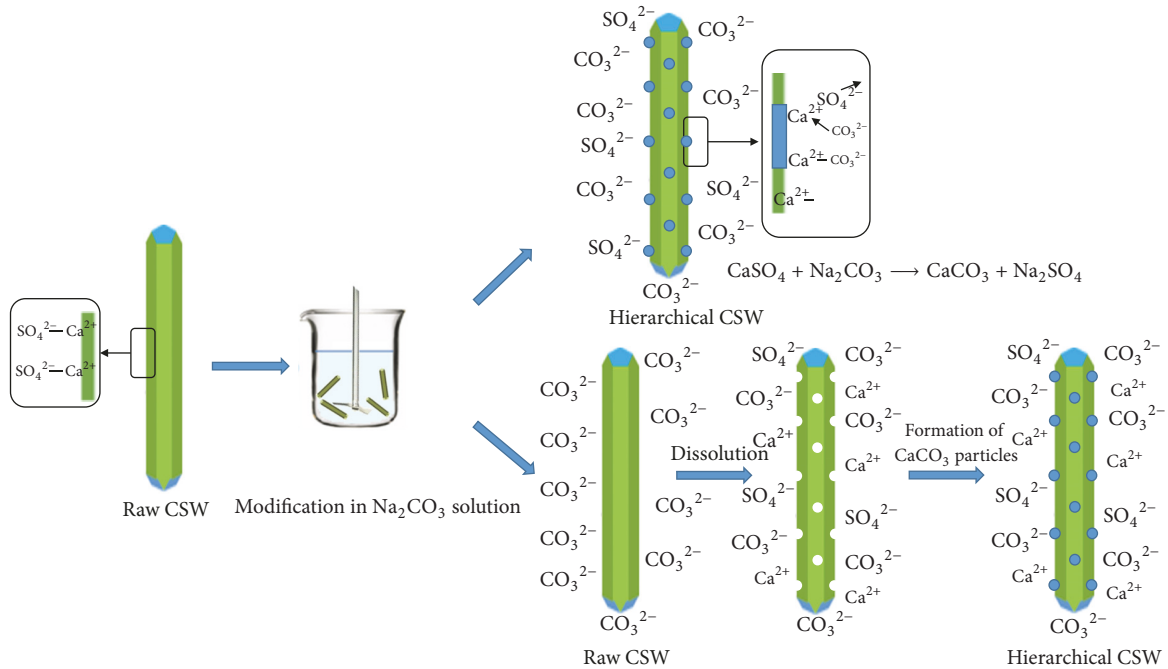


FIGURE 5: Schematic drawing for formation of hierarchical CSW in  $\text{Na}_2\text{CO}_3$  solution.

the PVC matrix if the crack extended through the composite (Figure 8(b)).

Based on the stress balance, the stress for the pull-out of the smooth whiskers can be expressed as follows:

$$P_1 = \frac{2\tau_e}{r}h, \quad (1)$$

where  $r$  was the radius of whisker,  $\tau_e$  was the interfacial shearing strength between whisker and PVC matrix, and  $h$  was the pull-out length of the whisker.

In the case of hierarchical CSW/PVC composite, the  $\text{CaCO}_3$  nanoparticles were considered to be distributed

uniformly on the surface of the hierarchical CSW (Figures 8(c) and 8(d)). On the basis of Kelvin model in the elastic mechanics, the pull-out stress of the hierarchical CSW from the PVC matrix can be expressed as follows:

$$P = P_1 + nP_2 = \frac{2\tau_e}{r}h + 16n\pi(1 - \nu_m)G_m wH,$$

$$H = \sqrt{a^2 - \frac{r'^2}{\left[ \frac{1}{3} \left( \sqrt{a^2 - r'^2}/a \right)^3 + (3 - 4\nu_m) \left( \sqrt{a^2 - r'^2}/a \right) \right]}} \quad (2)$$

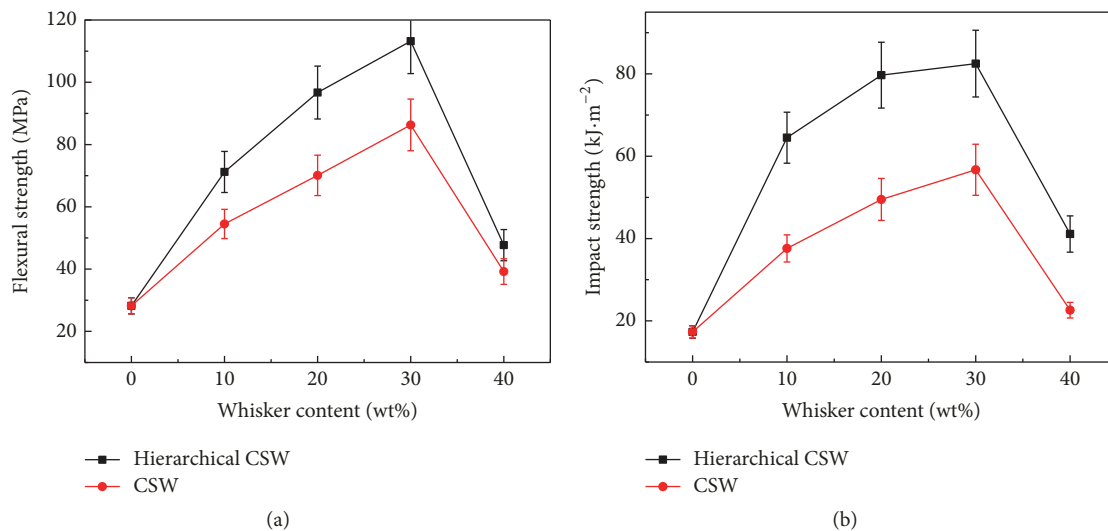


FIGURE 6: Flexural strength (a) and impact strength (b) of CSW/PVC and hierarchical CSW/PVC composites with different whisker content.

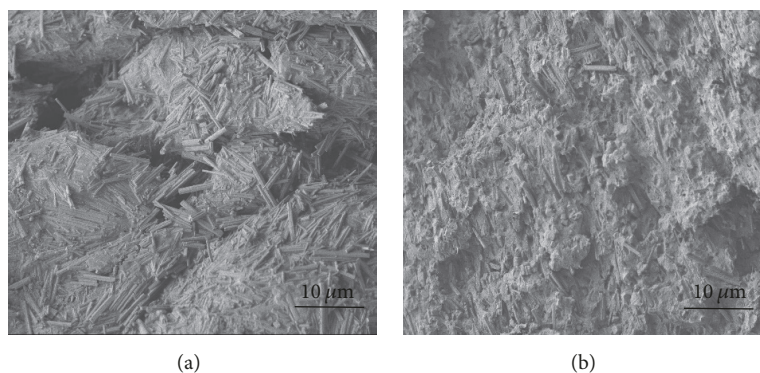


FIGURE 7: Fracture surface of CSW/PVC (a) and hierarchical CSW/PVC composites.

where  $w$  was the pull-out displacement along  $x$ -axis at point  $O$  as a result of the stress concentration  $P_2$ ,  $\nu_m$  and  $G_m$  were Poisson's ratio and shear modulus of PVC matrix,  $a$  was the distance between point  $O$  and point  $M$ ,  $r'$  was the horizontal distance between point  $M$  and the central axis of the whisker, and  $n$  was the number of the  $\text{CaCO}_3$  particles on CSW surface. The  $\text{CaCO}_3$  nanoparticles on CSW surface provided an excess pull-out stress ( $16n\pi(1 - \nu_m)G_m wH$ ) compared to the raw CSW, which improved the interfacial interaction between the hierarchical CSW and the PVC matrix, favoring the increase of mechanical properties of the composite.

The above experimental results and the interfacial analysis indicated that the hierarchical CSW with rough surface favored the mechanical interlocking between CSW and PVC matrix, producing CSW/PVC composite with high flexural strength and impact strength.

#### 4. Conclusions

Hierarchical CSW comprised of  $\text{CaCO}_3$  nanoparticles and CSW were prepared by modification of CSW in  $\text{Na}_2\text{CO}_3$  solution at  $80^\circ\text{C}$ . The coating of  $\text{CaCO}_3$  nanoparticles with an

average size of 50–100 nm on CSW surfaces led to the increase of the surface roughness of CSW from 56.8 nm to 115.6 nm. The hierarchical structure of CSW favored the mechanical interlocking between CSW and PVC matrix and the use of the hierarchical CSW rather than the raw CSW in the fabrication of CSW/PVC composite led to an increase of the flexural strength from 86.3 MPa to 113.2 MPa and the impact strength from  $56.7 \text{ kJ}\cdot\text{m}^{-2}$  to  $82.5 \text{ kJ}\cdot\text{m}^{-2}$ .

#### Conflicts of Interest

The authors declare that there are no conflicts of interest regarding the publication of this paper.

#### Acknowledgments

This work was supported by the National Science Foundation of China (nos. 51234003 and 51374138) and Key Scientific and Technical Project concerned with coal-bearing resources in Shanxi province (no. MC2014-06).

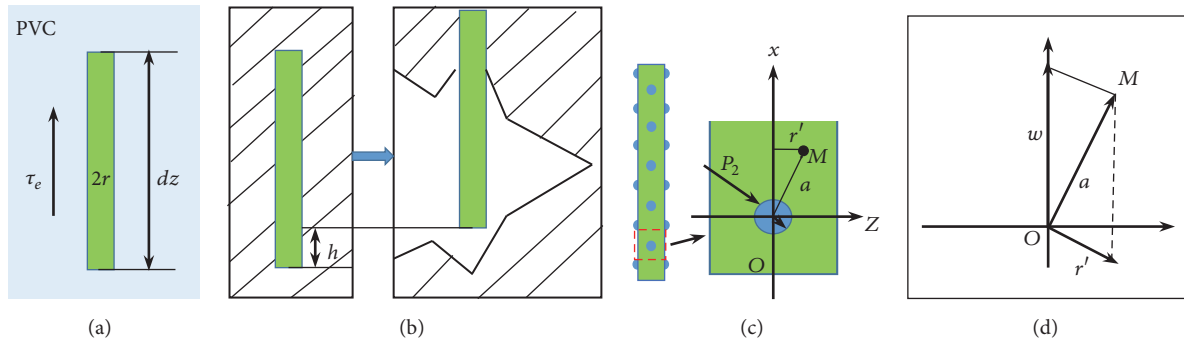


FIGURE 8: Micromechanical modeling of CSW/PVC composites (a, b) and hierarchical CSW/PVC composites (c, d).

## Supplementary Materials

The detailed formula derivation process of the interfacial analysis of CSW/PVC and hierarchical CSW/PVC composites in Section 3.3 was presented in the Supplementary Material. (*Supplementary Materials*)

## References

- [1] J. H. Jhaveri, C. M. Patel, and Z. V. P. Murthy, "Preparation, characterization and application of GO-TiO<sub>2</sub>/PVC mixed matrix membranes for improvement in performance," *Journal of Industrial and Engineering Chemistry*, vol. 52, pp. 138–146, 2017.
- [2] T. F. Silva, B. G. Soares, S. C. Ferreira, and S. Livi, "Silylated montmorillonite as nanofillers for plasticized PVC nanocomposites: Effect of the plasticizer," *Applied Clay Science*, vol. 99, pp. 93–99, 2014.
- [3] Z. Jiang, K. Yao, Z. Du, J. Xue, T. Tang, and W. Liu, "Rigid cross-linked PVC foams with high shear properties: The relationship between mechanical properties and chemical structure of the matrix," *Composites Science and Technology*, vol. 97, pp. 74–80, 2014.
- [4] H. Y. Chen, J. Wang, P. Y. Ma, J. Liang, and L. Xiang, "Influence of hydroxylation on fabrication of PVC/CaSO<sub>4</sub> composite," *Applied Surface Science*, vol. 357, pp. 2320–2326, 2015.
- [5] L. Madaleno, J. Schjødt-Thomsen, and J. C. Pinto, "Morphology, thermal and mechanical properties of PVC/MMT nanocomposites prepared by solution blending and solution blending+melt compounding," *Composites Science and Technology*, vol. 70, no. 5, pp. 804–814, 2010.
- [6] S. Sun, C. Li, L. Zhang, H. L. Du, and J. S. Burnell-Gray, "Interfacial structures and mechanical properties of PVC composites reinforced by CaCO<sub>3</sub> with different particle sizes and surface treatments," *Polymer International*, vol. 55, no. 2, pp. 158–164, 2006.
- [7] E. M. van der Merwe, C. L. Mathebula, and L. C. Prinsloo, "Characterization of the surface and physical properties of South African coal fly ash modified by sodium lauryl sulphate (SLS) for applications in PVC composites," *Powder Technology*, vol. 266, pp. 70–78, 2014.
- [8] S. Hou, J. Wang, X. Wang, H. Chen, and L. Xiang, "Effect of Mg<sup>2+</sup> on hydrothermal formation of  $\alpha$ -CaSO<sub>4</sub>·0.5H<sub>2</sub>O whiskers with high aspect ratios," *Langmuir*, vol. 30, no. 32, pp. 9804–9810, 2014.
- [9] Z. Zhu, L. Xu, G. Chen, and Y. Li, "Optimization on tribological properties of aramid fibre and CaSO<sub>4</sub> whisker reinforced non-metallic friction material with analytic hierarchy process and preference ranking organization method for enrichment evaluations," *Materials and Corrosion*, vol. 31, no. 1, pp. 551–555, 2010.
- [10] J. Y. Liu, L. Reni, Q. Wei et al., "Fabrication and characterization of polycaprolactone/calcium sulfate whisker composites," *Express Polymer Letters*, vol. 5, no. 8, pp. 742–752, 2011.
- [11] F. Dong, J. Liu, H. Tan, C. Wu, X. He, and P. He, "Preparation of calcium sulfate hemihydrate and application in polypropylene composites," *Journal of Nanoscience and Nanotechnology*, vol. 17, no. 9, pp. 6970–6975, 2017.
- [12] W. Yuan, J. Cui, Y. Cai, and S. Xu, "A novel surface modification for calcium sulfate whisker used for reinforcement of poly(vinyl chloride)," *Journal of Polymer Research*, vol. 22, no. 9, p. 173, 2015.
- [13] C. Liu, Q. Zhao, Y. Wang, P. Shi, and M. Jiang, "Surface modification of calcium sulfate whisker prepared from flue gas desulfurization gypsum," *Applied Surface Science*, vol. 360, pp. 263–269, 2016.
- [14] J. Cui, Y. Cai, W. Yuan, Z. Lv, and S. Xu, "Preparation of a Crosslinked Chitosan Coated Calcium Sulfate Whisker and Its Reinforcement in Polyvinyl Chloride," *Journal of Materials Science and Technology*, vol. 32, no. 8, pp. 745–752, 2016.
- [15] W. Yuan, Y. Lu, and S. Xu, "Synthesis of a new titanate coupling agent for the modification of calcium sulfate whisker in poly(vinyl chloride) composite," *Materials*, vol. 9, no. 8, p. 625, 2016.
- [16] X. Feng, Y. Zhang, G. Wang, M. Miao, and L. Shi, "Dual-surface modification of calcium sulfate whisker with sodium hexametaphosphate/silica and use as new water-resistant reinforcing fillers in papermaking," *Powder Technology*, vol. 271, pp. 1–6, 2015.
- [17] X. Jia, G. Li, B. Liu, Y. Luo, G. Yang, and X. Yang, "Multiscale reinforcement and interfacial strengthening on epoxy-based composites by silica nanoparticle-multiwalled carbon nanotube complex," *Composites Part A: Applied Science and Manufacturing*, vol. 48, no. 1, pp. 101–109, 2013.
- [18] C. Gu, X. Song, S. Zhang, S. O. Ryu, and J. Huang, "Synthesis of hierarchical  $\alpha$ -Fe<sub>2</sub>O<sub>3</sub> nanotubes for high-performance lithium-ion batteries," *Journal of Alloys and Compounds*, vol. 714, pp. 6–12, 2017.
- [19] P. I. Gonzalez-Chi, O. Rodríguez-Uicab, C. Martín-Barrera et al., "Influence of aramid fiber treatment and carbon nanotubes on the interfacial strength of polypropylene hierarchical composites," *Composites Part B: Engineering*, vol. 122, pp. 16–22, 2017.

- [20] L. Gao, Q. Zhang, M. Zhu, X. Zhang, G. Sui, and X. Yang, "Polyhedral oligomeric silsesquioxane modified carbon nanotube hybrid material with a bump structure via polydopamine transition layer," *Materials Letters*, vol. 183, pp. 207–210, 2016.
- [21] T. Zhao, B. Guo, F. Zhang, F. Sha, Q. Li, and J. Zhang, "Morphology Control in the Synthesis of CaCO<sub>3</sub> Microspheres with a Novel CO<sub>2</sub>Storage Material," *ACS Applied Materials & Interfaces*, vol. 7, pp. 15918–15927, 2015.



**Hindawi**  
Submit your manuscripts at  
[www.hindawi.com](http://www.hindawi.com)

